Ultrasound in Medicine & Biology 51 (2025) 280–287

Contents lists available at ScienceDirect

Ultrasound in Medicine & Biology

journal homepage: www.elsevier.com/locate/ultrasmedbio

Original Contribution

Ultrasound Speckle Tracking Method Based on Gradient Optical Flow to Quantify Small Longitudinal Displacement, Shear and Longitudinal Strain in Peripheral Nerves

Žiga Snoj [a,b], Gregor Omejec [c,d], Jaka Javh [e], Nejc Umek [f,*]

[a] Department of Radiology, Faculty of Medicine, University of Ljubljana, Ljubljana, Slovenia
[b] Clinical Institute of Radiology, University Medical Centre Ljubljana, Ljubljana, Slovenia
[c] Division of Neurology, Institute of Clinical Neurophysiology, University Medical Centre Ljubljana, Ljubljana, Slovenia
[d] The Higher Education Institution Fizioterapevtika, Medvode, Slovenia
[e] Motion Scope, Lukovica, Slovenia
[f] Faculty of Medicine, Institute of Anatomy, University of Ljubljana, Ljubljana, Slovenia

ARTICLE INFO

Keywords:
Speckle tracking
Gradient optical flow
High-resolution ultrasound
Peripheral nerve displacement
Shear strain quantification

ABSTRACT

Objective: This study aimed to develop, validate and test the clinical feasibility of ultrasound (US) speckle tracking method based on gradient optical flow for quantifying small longitudinal displacements, shear and strain in peripheral nerves.

Methods: The speckle tracking method was validated using seven thawed, fresh-frozen isolated cadaveric forearms. Longitudinal motion of the median nerve was captured using a high-frequency 22 MHz linear probe. An air bubble marker was inserted as a reference point for manual measurement comparison. The precision and accuracy of the method were assessed by comparing manual and automatic measurements. Clinical feasibility was tested on eight healthy subjects, measuring the longitudinal displacement of the median nerve during elbow extension and shoulder anteflexion.

Results: The method demonstrated linearity, high precision and accuracy, particularly with a backtrace of five frames, reducing the displacement underestimation to 4%. In cadaveric models, the highest shear strain was observed at the nerve-tissue interfaces. In healthy subjects, the mean displacement of the median nerve was 3.3 ± 1.0 mm, with good inter-rater reliability (intraclass correlation coefficient = 0.87).

Conclusion: The US speckle tracking method based on gradient optical flow effectively quantifies small longitudinal displacements and shear strain in peripheral nerves, with high precision and accuracy. However, the method could not detect longitudinal strain in nerves within the range of tested displacements. Future studies should investigate its applicability to smaller and deeper nerves and its usefulness in different pathological conditions.

Introduction

With advances in high-resolution ultrasound (US) technology and the utilization of high-frequency probes (20 MHz and above), nerve US has emerged as the gold standard for imaging peripheral nerves. This is primarily attributed to its excellent spatial resolution and the capability for dynamic imaging [1]. Because changes in the structural dispositions and biomechanics of peripheral nerves and surrounding tendons are known to correlate with the clinical severity of various entrapment neuropathies (i.e., carpal tunnel syndrome – CTS), US imaging has become an increasingly important tool for confirming clinically suspected entrapment neuropathies [2,3]. In addition to static US imaging, a few studies have utilized dynamic US imaging in patients with CTS, demonstrating the potential of dynamic assessment of the median nerve in these patients [4–6]. These studies assessed either transverse or longitudinal mobility of the median nerve at the wrist. The transverse mobility of the median nerve has been shown to be reduced in patients with CTS. However, due to the pathophysiological theory underlying this pathology, transverse mobility may not be as characteristic as longitudinal mobility. Few studies have investigated the possibility of using longitudinal mobility of the median nerve to increase the diagnostic accuracy of US examination in CTS. While these studies generally indicated a decrease in the longitudinal mobility of the median nerve at the wrist, the findings across the studies have been inconsistent [2,7–9]. These inconsistencies can be attributed to methodological variations and technical considerations when analysing longitudinal displacement using US videos.

Researchers have developed many different methods to estimate longitudinal nerve movement, including Doppler US [10], speckle tracking

* Corresponding author. Faculty of Medicine, Institute of Anatomy, University of Ljubljana, Slovenia, Korytkova ulica 2, 1000 Ljubljana, Slovenia.
E-mail address: nejc.umek@mf.uni-lj.si (N. Umek).

https://doi.org/10.1016/j.ultrasmedbio.2024.10.002
Received 12 June 2024; Revised 30 September 2024; Accepted 6 October 2024

with cross-correlation [11] and sum-absolute-difference [12] or velocity vector algorithms [13]. Cross-correlation methods are frequently utilized to track specific speckles within a restricted number of regions of interest inside the nerve tissue, primarily quantifying gross nerve movement [11,14–17]. These methods operate under the assumption that the nerve is a homogeneous structure undergoing movement as a single entity, thereby precluding the tracking of individual nerve layers. However, the nerve structure is not homogeneous but has a complex fascicular anatomy [18]. Consequently, the movement of longitudinal structures may not be uniform, as uneven displacements within the structure can occur [19]. These uneven displacements can generate shear forces between the moving layers of the structure or between the structure and its surrounding tissues [20]. Furthermore, these methods tend to be challenging to implement, often necessitating specialized hardware, advanced programming and mathematical expertise, and are quite time-consuming [11], rendering them unsuitable for routine clinical application. Accordingly, the aim of this study was to develop, validate and evaluate the clinical feasibility of a US full-field speckle tracking method based on gradient optical flow. This method is intended to visualize and quantify small longitudinal displacements, shear and longitudinal strains within peripheral nerves from US videos.

Materials and methods

The validation of our speckle tracking method was performed on cadavers, while the clinical feasibility testing was performed on healthy subjects. The study protocol was reviewed and approved by the Republic of Slovenia National Medical Ethics Committee (Permit No: 0120-538/2019/4).

Donated bodies

For the study, seven thawed, fresh-frozen, isolated forearms were utilized. These forearms were obtained from three male and four female cadavers, with an age range of 70–89 y. The bodies had been donated for research and educational purposes to the Institute of Anatomy, Faculty of Medicine, University of Ljubljana, through a willed cadaver donation program.

Imaging of nerve longitudinal motion

Longitudinal displacement of the median nerve was induced by slowly applying 20N of traction. This was achieved using a digital dynamometer (HF 1000, Nanbei Instrument Limited, Zhengzhou, China), which was securely fastened directly to the exposed proximal end of the nerve in the forearm (Fig. 1). The longitudinal motion of the median nerves was captured using an Aplio i800 US machine equipped with a high-resolution 22 MHz linear probe. The imaging was performed at 30 frames per second, with a pixel size of 48.3 × 16.2 μm. The linear probe was positioned perpendicular to the skin on the volar side of the distal forearm, just proximal to the wrist. It was oriented longitudinally along the median nerve and parallel to the direction of nerve motion. To facilitate the detection and measurement of nerve motion, an air bubble was introduced into the centre of the median nerve using a thin needle. This air bubble served as a marker in the US images. The raw US video, in DICOM file format and without any postprocessing, was exported for subsequent analyses.

Figure 1. Experimental setup for imaging nerve longitudinal motion in a cadaveric model.

Automatic speckle tracking method

Automatic speckle tracking of successive images of US video was performed with standard Motion-Scope Tracker software (Motion-Scope, Lukovica, Slovenia) using a gradient-based tracker for measuring displacements and deformations from videos and image sequences. To increase the accuracy of speckle tracking, the software was custom-tailored to enable backtracing of several frames (*vide infra*).

Motion tracking from images is feasible only in regions exhibiting high-intensity contrasts, as these areas demonstrate substantial intensity variations during movement. US images of tissues inherently generate speckles with sparse contrast. The software automatically identified regions with adequately high contrast and partitioned them into small kernels used for tracking. These kernels were not uniformly distributed but were positioned to capture the most pronounced contrast within specific image regions. The kernel size was set to 19 pixels, and the inter-kernel spacing was set to a maximum of 6 pixels to generate a dense displacement grid.

The tracking was derived from the minimization of error using local image intensity gradients for gradient descent between the first image $I_0(\mathbf{x})$ and the second image $I_1(\mathbf{x})$ shifted for $\mathbf{s}$, where $\mathbf{x}$ is the vector of image spatial coordinates $\mathbf{x}=\{x, y\}^T$ and $\mathbf{s}$ is the displacement vector $\mathbf{s}=\{s_x, s_y\}^T$. Although for tracking, it is possible to use a higher 6 degree-of-freedom displacement vector $\mathbf{s}$, the 2 degree-of-freedom vector $\{s_x, s_y\}^T$ was used to better determine the solution of the relatively sparse speckle pattern. The theoretical and mathematical basis of the method is explained in greater detail in Javh et al. [21].

Displacement measurements are typically most effectively conducted with respect to a common reference frame, I_0. However, due to unintentional alterations in US speckles caused by minor angle and motion shifts in the US section plane, an incremental tracking approach was employed. In incremental tracking, the reference frame for each frame (I_n) is the immediately preceding frame (I_{n-1}) rather than a consistent, common reference frame. To further improve the tracking consistency across the image sequence, a backtracing methodology was incorporated. This involved utilizing a set of multiple recent frames (backtrace frames) as the reference. The displacement between the current frame and each of the backtrace frames was added to the individual displacements of the respective backtrace frame, resulting in five distinct displacement estimations for the current frame. The final displacement for the current frame was computed as the mean of these five individual displacement estimates. In the scenario with a backtrace set at five, the displacements were determined by tracking the current frame relative to the five most recent frames, and the mean displacement was adopted as the outcome. In instances where the tracking error minimization failed to converge, the corresponding point was excluded from the tracking process.

The obtained displacement vector $\mathbf{s}$ produced by the error minimization was used to calculate shear strain γ_{xy} as:

$$\gamma_{xy} = \frac{\partial s_x}{\partial y} + \frac{\partial s_y}{\partial x}$$

Longitudinal strains ε_{xx}, ε_{yy} were calculated as:

$$\varepsilon_{xx} = \frac{\partial s_x}{\partial x},$$

$$\varepsilon_{yy} = \frac{\partial s_y}{\partial y}$$

The shear strain was normalized to the mean nerve displacements.

Assessment of automatic speckle tracking performance

The performance of the automatic speckle tracking was validated by determining linearity, precision and accuracy.

The precision of the automatic speckle tracking method was evaluated by measuring the displacements of the median nerve at six evenly spaced cross-sections, covering approximately 2 mm of the nerve's length. These measurements were taken at three different points of nerve displacement: one-third, two-thirds and at the point of maximal displacement during each movement of the median nerve (Fig. 2). For each displacement point, we compared the locations within the nerve where the measurements showed the greatest differences.

The linearity and accuracy of the automatic speckle tracking method were evaluated by comparing the manually measured displacements of the median nerves, marked by the air bubble, with the displacements automatically measured using the speckle tracking method at the same positions during longitudinal nerve motion. The manually measured displacements served as the absolute standard for comparison. To assess the linearity of the relationship between the manually measured and automatically tracked displacements, linear regression analysis was performed, and the coefficient of determination (R^2) was computed. To assess the accuracy, the slope of the linear regression curve was determined.

Given that the air bubble marker could potentially enhance speckle tracking performance by augmenting contrast, the automatic speckle tracking measurements were acquired a few millimetres away from the marker, in a region where the nerve's contrast was not artificially elevated (Fig. 2). To mitigate potential errors arising from the lower precision of the automatic speckle tracking, the average displacement was calculated from measurements obtained at six parallel points along the longitudinal axis of the nerve.

The shear and longitudinal strains were initially assessed semiquantitatively through careful examination of US videos depicting median nerve motion. In these images, strain was represented by colours: yellow signified positive strain, while blue indicated negative strain, with the colour intensity reflecting the magnitude of the strain. Following this visual analysis, a quantitative analysis was performed at the specific locations where the semi-quantitative analysis had revealed the most pronounced strain.

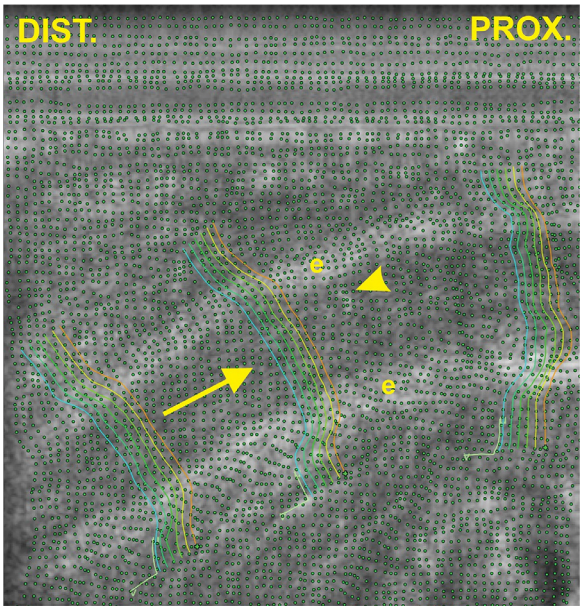

Figure 2. Tracked median nerve at a displacement of 1.2 mm to the right side of the image following the application of 20N of traction in a cadaveric model. Green dots represent the positions of the tracked kernels, while six parallel lines demarcate six consecutive cross-sections of the nerve, spanning approximately 2 mm of its length. The arrow illustrates the direction of movement, with the arrowhead pointing towards the air bubble marker, and the letter "e" denoting the epineurium. Frame width and depth is approximately 20 × 7 mm.

Evaluation of clinical feasibility of the automatic speckle tracking of median nerve longitudinal displacement in healthy subjects

Median nerve longitudinal displacement was measured bilaterally in four male and four female subjects aged 32 ± 2 y, using the same US machine, probe, and settings described above. All subjects provided informed consent prior to participation. The probe was positioned perpendicular to the skin and oriented longitudinally along the median nerve, just proximal to the wrist. US videos were acquired during the following maneuver: The forearm and wrist were maintained in a neutral position, with the elbow flexed at 90° and the upper arm parallel to the body. Subsequently, the elbow was extended to 180° while the upper arm was anteflexed to 90° over a duration of 10 s. This movement resulted in the proximal displacement of the median nerve. Throughout the maneuver, the neck was kept in a neutral position.

To determine the inter-rater reliability of median nerve longitudinal displacement measurements, each displacement was captured independently by two experienced ultrasonographers performing US nerve imaging in daily clinical practice. The maximal displacements of the nerve during the described movement were measured in raw US videos, utilizing a backtrace of five frames as detailed earlier. Additionally, shear strain at both the superficial and deep interfaces between the nerve and surrounding tissue was also quantified at displacements of 1 and 2 mm.

Statistical analysis

GraphPad Prism 10 (GraphPad Software, San Diego, CA, USA) was employed for all statistical analyses and graphical representations. The normality of data distribution was evaluated using the Kolmogorov–Smirnov test. Displacement measurements with a backtrace of one frame and a backtrace of five frames were compared using a paired *t*-test. Precision was assessed by comparing relative standard deviations. The relative standard deviations between different displacements within a single nerve were compared using repeated measures one-way ANOVA. Calibration equations were obtained, and slopes were compared using the least squares linear regression model. The linearity of models was assessed by the coefficient of determination (R^2). Shear strain at 1 and 2 mm displacements, as well as at the superficial and deep interfaces between the median nerve and surrounding tissue, were compared using a paired *t*-test. Displacements of the median nerve in healthy subjects, as measured by two sonographers in both the left and right hands, were compared using a paired *t*-test. Inter-rater agreement was assessed using the intraclass correlation coefficient (ICC), where ICC values ≥0.70 are considered satisfactory (0.91–1.0: excellent; 0.75–0.90: good; 0.51–0.74: moderate; below 0.50: poor) [22]. Data are presented as means ± standard deviations, and the difference was considered statistically significant at $p < 0.05$.

Results

Seven US videos of median nerve longitudinal movement in the distal forearm were analysed, following the slow application of 20N traction in a cadaveric model. The average maximum nerve displacement was 2.8 ± 0.9 mm (range 1.65–4.50 mm). The processing speed of the high-resolution US videos with a standard laptop (CPU – Intel Core i7-8565U) was approximately 4 s per 100 frames with a backtrace of one frame and approximately 25 s per 100 frames with a backtrace of five frames.

Precision

Repeated measures one-way ANOVA of the relative standard deviations demonstrated that the precision of automatic speckle tracking for longitudinal median nerve movement increased with larger displacements. This trend was observed for both a backtrace of one frame ($p = 0.036$) and five frames ($p = 0.037$). Utilizing a backtrace of five frames significantly improved precision compared to a backtrace of one frame (Table 1). The highest precision was noted for nerve 1, while nerve 2 exhibited the lowest.

Accuracy

Correlation between automatic speckle tracking of longitudinal movement and manual measurements of median nerve marker displacement showed good linearity over the entire displacement range of 0 −4.50 mm (Fig. 3). Automatic speckle tracking with a backtrace of one frame underestimated the true displacement by 13% ± 5%, whereas automatic speckle tracking with a backtrace of five frames was significantly better and underestimated the true displacement by 4% ± 4%. The accuracy of automatic speckle tracking was highest for nerve 4 and lowest for nerve 3 (Table 2).

Shear strain

Semi-quantitative analysis utilizing colour coding demonstrated that during longitudinal displacement of the nerve, the highest shear strain is localized at the interface between the median nerve and the surrounding tissue. Lower levels of shear strain were also observed within the nerve itself, manifesting as longitudinal bands parallel to the nerve's orientation (Fig. 4). Quantitative analysis of the shear strain at the interface between the median nerve and the surrounding tissue at displacements of 0.5, 1.0 and 1.5 mm revealed that shear strain increased with larger nerve displacements. Additionally, at displacements of 0.5 and 1.0 mm, shear strain was significantly elevated at the deep interface compared to the superficial interface. At the deep interface, the shear strain normalized to displacement was significantly higher for small displacements in comparison to large displacements (Table 3).

Longitudinal strain

Semi-quantitative analysis of longitudinal strain in the direction of median nerve movement revealed multiple parallel bands exhibiting low longitudinal strain in opposing directions, both at smaller and larger displacements, measuring up to 0.2 (Fig. 5). Consequently, further quantitative analysis was not pursued.

Longitudinal displacement of the median nerve in healthy subjects

Extension of the elbow with simultaneous anteflexion of the upper arm in eight young, healthy subjects bilaterally resulted in a proximal displacement of the median nerve averaging 3.3 ± 1.0 mm, with minimum and maximum displacements of 1.7 and 5.0 mm, respectively ($n = 16$) (Fig. 6). No significant differences were observed between the left and right sides ($p = 0.19$) or between male and female subjects ($p = 0.99$). Inter-rater reliability between the two sonographers was good, with an ICC of 0.87 (95% CI 0.68–0.95).

The normalized shear strain at 1 mm and 2 mm displacements of the median nerve was 2.14 ± 0.69 mm^{-1} and 2.27 ± 0.67 mm^{-1} for the superficial interface, and 2.21 ± 0.75 mm^{-1} and 2.37 ± 0.66 mm^{-1} for the deep interface between the median nerve and surrounding tissue, respectively. No significant differences were found between normalized shear strain at 1 mm and 2 mm displacements ($p = 0.25$ for superficial and $p = 0.25$ for deep interface), between normalized shear strain at the superficial and deep interfaces ($p = 0.44$), or between the left and right upper extremities ($p = 0.097$).

Discussion

In this study, we successfully developed and evaluated a US speckle tracking method based on gradient optical flow for the quantification of small longitudinal displacements, shear and strain in peripheral nerves. Our findings demonstrate that this method is capable of automatically tracking and measuring longitudinal displacements of the median nerve up to 4.5 mm with satisfactory precision and accuracy. We further observed that precision can be enhanced by increasing the backtrace of frames, although this comes at the cost of increased computational demands and processing time. The method also proved effective in detecting shear strain at the interface between the median nerve and the surrounding tissue. However, it was not sufficiently robust to detect small longitudinal strain within the median nerve itself. Clinical testing in young, healthy subjects confirmed that measuring the longitudinal displacement of the median nerve at the wrist using this method is both feasible and reliable in a clinical setting, demonstrating good inter-rater reliability.

We validated our speckle tracking method up to a median nerve displacement of 4.5 mm. This range encompasses the majority of manually measured median nerve displacements in the upper arm, median nerve displacements during finger, wrist, and elbow flexion reported by McLellan et al. [23], and ultrasonographically measured median nerve displacements in the forearm during wrist extension and elbow flexion observed by Dilley et al. [24]. The measurements demonstrated excellent linearity across the entire range of displacements, suggesting consistent accuracy. Consequently, the method is likely to perform well even

Table 1
Relative Standard Deviations (RSD, %) of the Measured Displacements for the Automatic Speckle Tracking of the Median Nerve in the Cadaveric Model, Calculated Across Six Parallel Nerve Regions at Three Different Displacement Levels: One-Third of the Maximum Displacement (1/3), Two-Thirds of the Maximum Displacement (2/3) and the Maximum Displacement (3/3)

	1/3 of Max. Displacement		2/3 of Max. Displacement		Max. Displacement		Average	
Nerve	Backtrace 1	Backtrace 5	Backtrace 1	Backtrace 5	Backtrace 1	Backtrace 5	Backtrace 1	Backtrace 5
1	4.5	2.6	3.6	1.7	3.2	2.3	3.8 ± 0.5	2.2 ± 0.3
2	16.9	14.2	16.9	12.4	14.1	11.3	16.0 ± 1.3	12.6 ± 1.2
3	23.5	5.9	12.6	2.8	11.4	2.8	15.9 ± 5.5	3.8 ± 1.5
4	17.5	13.5	6.4	9.2	8.7	3.8	10.8 ± 4.8	8.8 ± 4.0
5	9.1	4.4	5.7	2.9	2.6	3.4	5.8 ± 2.7	3.6 ± 0.6
6	11.1	5.4	9.5	5.6	10.5	3.9	10.4 ± 0.6	5.0 ± 0.8
7	13.7	4.7	13.7	2.4	11.4	1.6	13.0 ± 1.1	2.9 ± 1.3
Average	**13.8 ± 5.8**[a]	**7.2 ± 4.3**	**9.8 ± 5.3**	**5.3 ± 3.8**[a]	**8.8 ± 4.0**	**4.2 ± 3.0**[a]	**10.8 ± 4.3**	**5.6 ± 3.5**[a]

[a] $p < 0.05$ backtrace of one frame vs. backtrace of five frames (paired *t*-test).

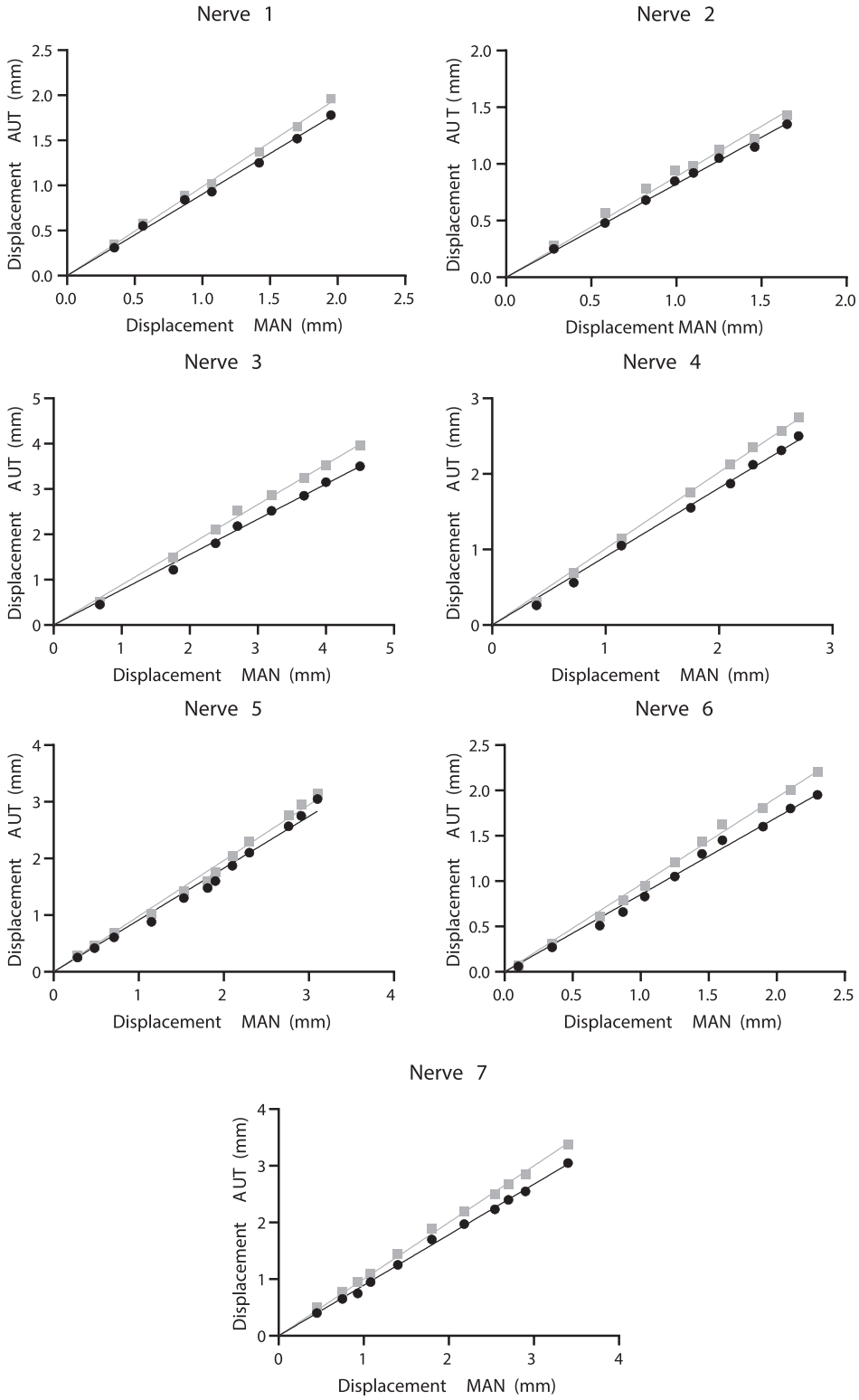

Figure 3. Linear correlation between the manually (MAN) measured displacement of the median nerve in a cadaveric model using an air bubble as a marker (*x*-axis) and the automatically (AUT) measured displacement of the median nerve using automatic speckle tracking with a backtrace of one frame (black) and a backtrace of five frames (grey).

with larger displacements. The precision of the automatic displacement measurements was observed to be higher at larger displacements. This implies that when measuring very small displacements, it is advisable to measure displacements at multiple regions of interest within the nerve and average the results to achieve the most precise measurements. This averaging process can be automated within the software.

The accuracy of the displacement measurements was deemed sufficient. Automatic speckle tracking with a backtrace of one frame underestimated the true displacement by 13%, whereas automatic speckle tracking with a backtrace of five frames underestimated the true displacement by only 4%. This underestimation remained consistent across the entire range of displacements, suggesting that measurements

Table 2
Coefficients of Determination (R^2) and Slopes of the Calibration Curves for the Automatic Speckle Tracking Displacement Measurements of the Median Nerve in the Cadaveric Model Following the Application of a 20N Traction Force

	R^2		Slope		
Nerve	Backtrace 1	Backtrace 5	Backtrace 1	Backtrace 5	*p* Value[a]
1	0.99	0.99	0.90 CI (0.88–0.93)	0.99 CI (0.96–1.00)	<0.0001
2	0.99	0.98	0.82 CI (0.80–0.84)	0.89 CI (0.85–0.93)	0.0032
3	0.99	0.99	0.78 CI (0.76–0.80)	0.89 CI (0.87–0.90)	<0.0001
4	0.99	0.99	0.91 CI (0.88–0.93)	1.0 CI (0.99–1.02)	<0.0001
5	0.98	0.99	0.91 CI (0.88–9.5)	0.98 CI (0.95–1.01)	0.0044
6	0.99	0.99	0.85 CI (0.82–0.88)	0.96 CI (0.94–0.98)	<0.0001
7	0.99	0.99	0.89 CI (0.88–0.91)	0.99 CI (0.98–1.01)	<0.0001
Average	**0.9933 ± 0.0039**	**0.9940 ± 0.0056**	**0.87 ± 0.05**	**0.96 ± 0.04**	**<0.0001**

[a] Comparison of slope of backtrace of five frames vs. backtrace of one frame (paired *t*-test).

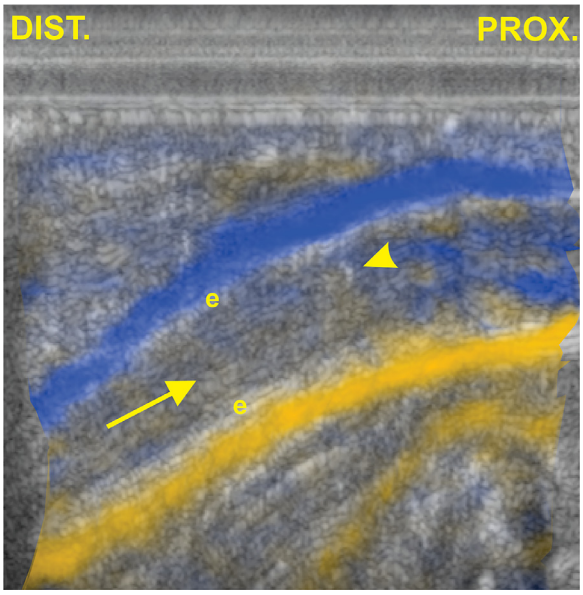

Figure 4. Colour-coded representation of the calculated shear strain within the median nerve of a cadaveric model at a displacement of 1.2 mm, ranging from 0 to 3.24. Blue denotes negative values, whereas yellow signifies positive values. The arrow indicates the direction of movement, with the arrowhead pointing towards the air bubble marker, and the letter "e" marking the epineurium. Frame width and depth is approximately 20 × 7 mm.

obtained using the same method are relatively comparable. Nevertheless, this underestimation should be taken into account when comparing results with those obtained using other methods or when reporting absolute measurements. The superior performance observed with backtracing of five frames is anticipated, as, unlike tracking based on a fixed reference frame [25], the reference frame undergoes continuous change during iterative tracking, leading to an accumulation of tracking errors. However, this strategy employed to mitigate tracking errors came at the expense of a 6.6-fold increase in processing time. Nonetheless, the processing time for each video remained under 1 min, rendering this method applicable in clinical settings where the speed of image processing is a crucial consideration.

We demonstrated that shear strain was most pronounced at both the superficial and deep interfaces between the median nerve and the surrounding tissue. The absolute magnitude of shear strain is influenced by the displacement. Therefore, we normalized it to the displacement value to facilitate comparison across different displacement values and subjects. In the cadaver model, the normalized shear strain remained constant at the superficial interface, suggesting consistent sliding of the nerve relative to its immediate surrounding tissue. Conversely, at the deep interface, normalized shear strain decreased with increasing displacement, implying that at larger displacements, the surrounding tissue also moved in conjunction with the nerve. In young, healthy subjects, normalized shear strain remained constant at both the deep and superficial interfaces during elbow extension and shoulder anteflexion. The observed discrepancies between the cadaver model and the young, healthy subjects could be attributed to inherent differences in nerve movement mechanics or postmortem changes in the cadaveric tissues [26].

Within the nerve, we observed lower levels of shear strain in the form of longitudinal bands running parallel to the nerve (Fig. 5). These bands may represent small shear strain between the multiple fascicles within the nerve [18]. At the nerve's origin, fascicles tend to straighten prior to stretching when subjected to loading [27], potentially generating this observable shear strain within the nerve. It is also conceivable that this could be attributed to artefacts. Therefore, further investigation on monofascicular nerves is warranted. Our method was evaluated solely on the median nerve, which is relatively large and superficially located on the distal forearm. Consequently, additional studies are necessary to assess its applicability to smaller and deeper nerves. During the visualization of longitudinal strain, multiple parallel bands with very small strain appeared throughout the visual field, oriented parallel to

Table 3
Absolute and Normalized Shear Strain at the Superficial and Deep Interfaces Between the Median Nerve and Surrounding Tissue, Measured at 0.5, 1.0 and 1.5 mm Longitudinal Displacements in a Cadaveric Model

	Superficial		Deep		*p* Value[a]
Displacement (mm)	Absolute Shear	Shear Strain/Displacement (mm^{-1})	Absolute Shear	Shear Strain/Displacement (mm^{-1})	
0.5	1.06 ± 0.22	2.13 ± 0.43	1.33 ± 0.27	2.65 ± 0.53	0.0195
1.0	2.02 ± 0.20	2.02 ± 0.20	2.40 ± 0.35	2.40 ± 0.35	0.0081
1.5	2.91 ± 0.55	1.94 ± 0.35	3.10 ± 0.49	2.06 ± 0.33	0.5040
p Value[b]	0.0002	0.4954	<0.0001	0.0422	

[a] Deep vs. superficial interface (paired *t*-test).
[b] Displacement effect on shear strain (repeated measures ANOVA).

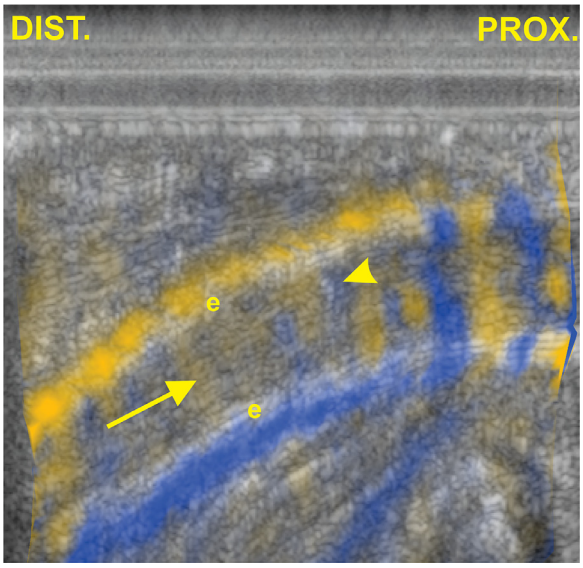

Figure 5. Colour-coded representation of the calculated longitudinal strain within the median nerve of a cadaveric model at a displacement of 1.2 mm, ranging from 0 to 0.40. Blue denotes negative values, whereas yellow signifies positive values. The arrow indicates the direction of movement, with the arrowhead pointing towards the air bubble marker, and the letter "e" marking the epineurium. Frame width and depth is approximately 20 × 7 mm.

the US beam. We hypothesize that this limitation could be due to the presence of fine acoustic shadow artefacts. These artefacts alter the intensity of speckles passing through the shadows, leading to minor errors that create the illusion of slight motion and deformation. Given that longitudinal strain in the median nerve during sliding is very low,

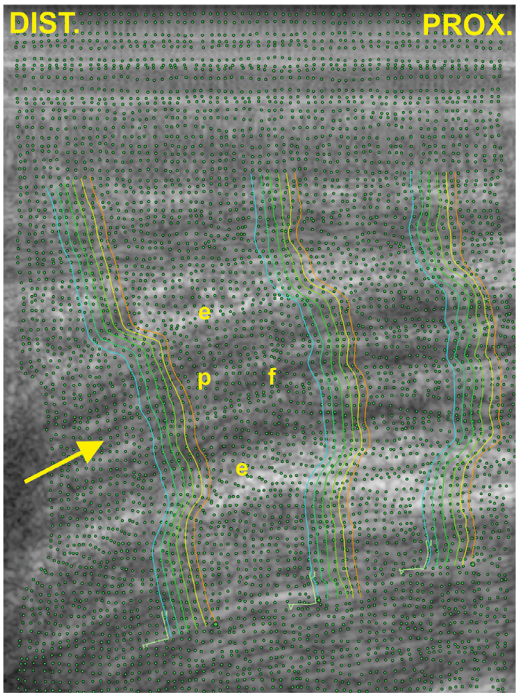

Figure 6. Tracked median nerve displacement of 2.0 mm following elbow extension and shoulder anteflexion in a young, healthy subject. Green dots indicate the traced kernels, while six parallel lines represent six consecutive cross-sections of the nerve, spanning approximately 2 mm of its length. The arrow denotes the direction of movement, "e" marks the epineurium, "f" marks a nerve fascicle and "p" marks the perineurium. Frame width and depth is approximately 20 × 8.5 mm.

ranging from 0.5% to 3.0% [24], our method was likely not sensitive enough to detect it.

The clinical applicability of the proposed method was tested in eight healthy volunteers, and the mean displacement of the median nerve during elbow extension and shoulder anteflexion was found to be 3.3 ± 1.0 mm. This finding is comparable to the measurements reported by Dilley et al. [24], who observed a displacement of 3.0 ± 1.0 mm for the median nerve at mid-forearm during elbow flexion up to 90°. The good agreement between the two sonographers in our study indicates that the median nerve displacement measurement using this method exhibits sufficient repeatability.

Our speckle tracking method possesses the capability to track all motions within the entire field of view concurrently. This feature is advantageous as multiple tissues (e.g., the median nerve and adjacent tendons) often undergo simultaneous movement during various actions. Furthermore, this capability enables us to compare the movements of different structures relative to one another and to compute the shear strain between adjacent structures.

Speckle tracking methods have some limitations. In the context of large displacements, US image tracking methods are constrained by the width of the field of view, which is dictated by the dimensions of the US probe. Conversely, for very small displacements, speckle tracking methods are limited in the transverse direction by the width of the US beam. Tracking is feasible only in regions exhibiting sufficient intensity contrast, which may be lacking in deep structures, particularly in obese patients and behind areas of partial acoustic shadowing where the US beam experiences significant attenuation. Optimal tracking can be achieved only when the probe is perfectly aligned parallel to the direction of movement. In all other scenarios, the displacement measurement will be underestimated.

Conclusion

We successfully developed and validated a US speckle tracking method based on gradient optical flow for the quantification of small longitudinal displacements, shear and strain in peripheral nerves. The method exhibited high precision and accuracy, especially when utilizing a backtrace of five frames, rendering it clinically viable. It effectively detected shear strain at the interface between the nerve and surrounding tissue but could not detect longitudinal strain within the nerve itself. While our primary focus was on the median nerve, future studies should investigate the applicability of this method to other nerves and in the context of various pathological conditions.

Conflict of interest

J.J. is the founder of Motion Scope and developer of the Motion-Scope Tracker software. The remaining authors declare no competing interests.

Acknowledgements

We are grateful to Chiedozie Kenneth Ugwoke, M.D., for his critical review of the manuscript. The study was funded by Slovenian Research and Innovation Agency Grant No. J3-4507 and P3-0043.

Data availability statement

The data generated and analysed during this study are available upon reasonable request to the corresponding author.

References

[1] Aseem F, Williams JW, Walker FO, Cartwright MS. Neuromuscular ultrasound in patients with carpal tunnel syndrome and normal nerve conduction studies. Muscle Nerve 2017;55(6):913–5.

[2] Filius A, Scheltens M, Bosch HG, Van Doorn PA, Stam HJ, Hovius SER, et al. Multidimensional ultrasound imaging of the wrist: changes of shape and displacement of the median nerve and tendons in carpal tunnel syndrome. J Orthop Res 2015;33(9):1332–40.
[3] Rossetto G, Lopomo NF, Shaikh SZ. Longitudinal movements and stiffness of lower extremity nerves measured by ultrasonography and ultrasound elastography in symptomatic and asymptomatic populations: a systematic review with meta-analysis. Ultrasound Med Biol 2023;49(9):1913–29.
[4] Park GY, Kwon DR, Seok JI, Park DS, Cho HK. Usefulness of ultrasound assessment of median nerve mobility in carpal tunnel syndrome. Acta Radiol 2018;59(12):1494–9.
[5] Kuo TT, Lee MR, Liao YY, Chen JP, Hsu YW, Yeh CK. Assessment of median nerve mobility by ultrasound dynamic imaging for diagnosing carpal tunnel syndrome. PLoS One 2016;11(1):e0147051.
[6] Stoianov AG, Patrascu JM, Hogea BG, Andor B, Florescu S, Jr JMP, et al. Static and dynamic ultrasound evaluation of the median nerve morphopathology in carpal tunnel syndrome diagnosis. Maedica (Bucur) 2022;17:591–5.
[7] Hough AD, Moore AP, Jones MP. Reduced longitudinal excursion of the median nerve in carpal tunnel syndrome. Arch Phys Med Rehabil 2007;88(5):569–76.
[8] Korstanje JWH, Boer MS De, Blok JH, Amadio PC, Hovius SER, Stam HJ, et al. Ultrasonographic assessment of longitudinal median nerve and hand flexor tendon dynamics in carpal tunnel syndrome. Muscle Nerve 2012;45(5):721–9.
[9] Erel E, Dilley A, Greening J, Morris V, Cohen B, Lynn B. Longitudinal sliding of the median nerve in patients with carpal tunnel syndrome. J Hand Surg Am 2003;28 B (5):439–43.
[10] Hough AD, Moore AP, Jones MP. Peripheral nerve motion measurement with spectral Doppler sonography: a reliability study. J Hand Surg Am 2000;25 B(6):585–9.
[11] Dilley A, Greening J, Lynn B, Leary R, Morris V. The use of cross-correlation analysis between high-frequency ultrasound images to measure longitudinal median nerve movement. Ultrasound Med Biol 2001;27(9):1211–8.
[12] Bohs LN, Trahey GE. A novel method for angle independent ultrasonic imaging of blood flow and tissue motion. IEEE Trans Biomed Eng 1991;38(3):280–6.
[13] Yeung F, Levinson SF. Feature-adaptive motion tracking of ultrasound image sequences using a deformable mesh. IEEE Trans Med Imaging 1998;17(6):945–56.
[14] Ellis RF, Hing WA, McNair PJ. Comparison of longitudinal sciatic nerve movement with different mobilization exercises: an in vivo study utilizing ultrasound imaging. J Orthop Sports Phys Ther 2012;42(8):667–75.
[15] Carroll M, Yau J, Rome K, Hing W. Measurement of tibial nerve excursion during ankle joint dorsiflexion in a weight-bearing position with ultrasound imaging. J Foot Ankle Res 2012;5(1):5.
[16] Boyd BS, Gray AT, Dilley A, Wanek L, Topp KS. The pattern of tibial nerve excursion with active ankle dorsiflexion is different in older people with diabetes mellitus. Clin Biomech 2012;27(9):967–71.
[17] Kasehagen B, Ellis R, Mawston G, Allen S, Hing W. Assessing the reliability of ultrasound imaging to examine radial nerve excursion. Ultrasound Med Biol 2016;42 (7):1651–9.
[18] Snoj Ž, Serša I, Maticic U, Cvetko E, Omejec G. Nerve fascicle depiction at MR microscopy and high-frequency us with anatomic verification. Radiology 2020;297 (3):672–4.
[19] Slane LC, Thelen DG. Non-uniform displacements within the Achilles tendon observed during passive and eccentric loading. J Biomech 2014;47(12): 2831–5.
[20] Yoshii Y, Villarraga HR, Henderson J, Zhao C, An KN, Amadio PC. Speckle tracking ultrasound for assessment of the relative motion of flexor tendon and subsynovial connective tissue in the human carpal tunnel. Ultrasound Med Biol 2009;35 (12):1973–81.
[21] Javh J, Slavič J, Boltežar M. The subpixel resolution of optical-flow-based modal analysis. Mech Syst Signal Process 2017;88:89–99.
[22] Bobak CA, Barr PJ, O'Malley AJ. Estimation of an inter-rater intra-class correlation coefficient that overcomes common assumption violations in the assessment of health measurement scales. BMC Med Res Methodol 2018;18(1):1–11.
[23] McLellan DL, Swash M. Longitudinal sliding of the median nerve during movements of the upper limb. J Neurol Neurosurg Psychiatry 1976;39(6):566–70.
[24] Dilley A, Lynn B, Greening J, DeLeon N. Quantitative in vivo studies of median nerve sliding in response to wrist, elbow, shoulder and neck movements. Clin Biomech 2003;18(10):899–907.
[25] Javh J, Slavič J, Boltežar M. Experimental modal analysis on full-field DSLR camera footage using spectral optical flow imaging. J Sound Vib 2018;434:213–20.
[26] Blumenthal S, Herskovitz S, Verghese J. Carpal tunnel syndrome in older adults. Muscle Nerve 2006;34(1):78–83.
[27] Kwan MK, Wall EJ, Massie J, Garfin SR. Strain, stress and stretch of peripheral nerve rabbit experiments in vitro and in vivo. Acta Orthop 1992;63(3):267–72.